



Multimodal brain predictors of current weight and weight gain in children enrolled in the ABCD study [®]

Shana Adise ^{a,*}, Nicholas Allgaier ^a, Jennifer Laurent ^c, Sage Hahn ^b, Bader Chaarani ^a, Max Owens ^a, DeKang Yuan ^b, Philip Nyugen ^{a,b,c,d}, Scott Mackey ^a, Alexandra Potter ^a, Hugh P. Garavan ^{a,d}

^a Department of Psychiatry, University of Vermont, Burlington, VT, USA

^b Department of Complex Systems, University of Vermont, Burlington, VT, USA

^c Department of Nursing, University of Vermont, Burlington, VT, USA

^d Department of Psychological Science, University of Vermont, Burlington, VT, USA

ARTICLE INFO

Keywords:

fMRI
Machine-learning
Childhood obesity
Reward
Inhibitory control
Weight gain
Weight stability

ABSTRACT

Multimodal neuroimaging assessments were utilized to identify generalizable brain correlates of current body mass index (BMI) and predictors of pathological weight gain (i.e., beyond normative development) one year later. Multimodal data from children enrolled in the Adolescent Brain Cognitive Development Study[®] at 9-to-10-years-old, consisted of structural magnetic resonance imaging (MRI), diffusion tensor imaging (DTI), resting state (rs), and three task-based functional (f) MRI scans assessing reward processing, inhibitory control, and working memory. Cross-validated elastic-net regression revealed widespread structural associations with BMI (e.g., cortical thickness, surface area, subcortical volume, and DTI), which explained 35% of the variance in the training set and generalized well to the test set ($R^2 = 0.27$). Widespread rsfMRI inter- and intra-network correlations were related to BMI ($R^2_{\text{train}} = 0.21$; $R^2_{\text{test}} = 0.14$), as were regional activations on the working memory task ($R^2_{\text{train}} = 0.20$; $R^2_{\text{test}} = 0.16$). However, reward and inhibitory control tasks were unrelated to BMI. Further, pathological weight gain was predicted by structural features (Area Under the Curve (AUC)_{train} = 0.83; AUC_{test} = 0.83, $p < 0.001$), but not by fMRI nor rsfMRI. These results establish generalizable brain correlates of current weight and future pathological weight gain. These results also suggest that sMRI may have particular value for identifying children at risk for pathological weight gain.

1. Introduction

Obesity is associated with a myriad of health consequences that increase mortality rates (Kelsey et al., 2014). In the United States, childhood obesity rates are near 19 % (Hales, 2017), while 70 % of the adult population is either overweight or obese (Fryar et al., 2018). Obesity rates may remain a public health concern for the foreseeable future as the complex blend of heritable (Vainik et al., 2018), behavioral and environmental factors (e.g., food-cues, obesogenic home environments, access to healthy foods and activities)(Gurnani et al., 2015; Hemmingson, 2018; Schempf et al., 2018) play a role its initiation and

maintenance. Obesity stems from myriad behaviors and causes, but overeating combined with decreased energy expenditure are the largest contributors (Hill et al., 2012). Under ideal circumstances, the brain tightly regulates food intake (Berthoud et al., 2012), but hedonic (i.e., reward) mechanisms can override appetitive homeostasis, and contribute to overeating and subsequent weight gain. Because the brain plays such a critical role in food intake mechanisms, understanding the associations between childhood obesity and the brain structure and function may benefit intervention programs targeted at changing behavior. Currently, there is little consistency regarding the relationships between childhood obesity and brain structure and function. A

Abbreviations: ABCD Study[®], Adolescent Brain Cognitive Development; AUC, Area under the curve; BMI, Body mass index; BOLD, Blood-oxygen-level-dependent; DTI, Diffusion tensor imaging; EN-back, Emotional N-back; FA, fractional anisotropy; fMRI, Functional magnetic resonance imaging; MD, Mean diffusivity; MID, Monetary Incentive Delay; ROI, Region of interest; rsfMRI, Resting state functional magnetic resonance imaging; SST, Stop Signal Task; WS, Weight stability; WG, Weight gain; Y1, year 1.

* Corresponding author at: Shana Adise, 1 South Prospect Street, Burlington, VT, 05401, USA.

E-mail address: sadise@chla.usc.edu (S. Adise).

<https://doi.org/10.1016/j.dcn.2021.100948>

Received 13 August 2020; Received in revised form 20 December 2020; Accepted 22 March 2021

Available online 30 March 2021

1878-9293/© 2021 Published by Elsevier Ltd. This is an open access article under the CC BY-NC-ND license (<http://creativecommons.org/licenses/by-nc-nd/4.0/>).

clearer understanding of these relationships will be pivotal for weight-related intervention programs.

Structural (s) and functional (f) magnetic resonance imaging (MRI) studies have associated childhood obesity to differences in brain anatomy (e.g., cortical thickness (Laurent et al., 2019), total gray matter volume (Mestre et al., 2017; de Groot et al., 2017; Alosco et al., 2014; Ronan et al., 2019; Perlaki et al., 2018; Rapuano et al., 2017), white matter architecture (Carbine et al., 2019; Geserick et al., 2018)), and altered functioning between networks at rest (Black et al., 2014; Moreno-Lopez et al., 2016) and, in response to rewarding stimuli in regions implicated in reward (Yokum et al., 2014a; Bohon, 2017; Batterink et al., 2010; Bruce et al., 2010) and inhibitory control (Bruce et al., 2010; Davids et al., 2010; Bruce et al., 2013; Van et al., 2016). However, inconsistent findings are a hallmark of MRI studies investigating childhood obesity with some studies finding differences in broad cortical brain territories, like the frontal cortex (Laurent et al., 2019; Alosco et al., 2014; Ronan et al., 2019; Carbine et al., 2019), or specific subcortical structures such as the hippocampus (Mestre et al., 2017), pallidum (de Groot et al., 2017), amygdala and accumbens (Perlaki et al., 2018; Rapuano et al., 2017), while others report no relationships (de Groot et al., 2017; Alosco et al., 2014; Sharkey et al., 2015). There have also been inconsistent fMRI findings. Differences in blood-oxygen-level-dependent (BOLD) response by weight status have been observed in prefrontal and orbitofrontal cortices (Batterink et al., 2010; Bruce et al., 2010), inferior frontal gyrus (Bruce et al., 2013; Van et al., 2016), insula (Bohon, 2017; Boutelle et al., 2015), amygdala (Boutelle et al., 2015), or not at all (Adise et al., 2018; Adise et al., 2019). Additionally, the directionality of effects has varied. Childhood obesity has been related to an imbalance between reward and inhibitory control (Burger and Berner, 2014), hyperfunctioning (Bohon, 2017; Boutelle et al., 2015; Kroemer and Small, 2016), and hypofunctioning (Batterink et al., 2010; Van et al., 2016; Stice and Yokum, 2016) of reward and inhibitory control networks. Discrepancies across studies muddles the interpretation of findings, which may hinder the development of treatment options in children.

Insufficient consistency across studies in identifying reliable and reproducible neural correlates (Turner et al., 2018) of childhood obesity may be due in part to historically small samples ($N < 100$) with homogeneous populations. In addition, differences in experimental paradigms and/or using different cohorts to test each modality (e.g., reward processing, inhibitory control) may further add to replication issues. To our knowledge, no studies have used the same cohort to investigate how childhood obesity relates to differences in the neural circuitry across various modalities (e.g., structure and function) and tasks (e.g., reward, inhibitory control). In addition, given the unreliability of the effects reported in the literature, it is currently unknown if any differences in sMRI or fMRI are reliable and robust enough for diagnostic and prognostic purposes. Understanding which brain functions and regions relate to childhood obesity may have particular benefit for developing successful prevention and intervention programs to target specific behavior changes. In addition, prevention programs may benefit from having a diagnostic tool to assess obesity risk in children prior to excess weight gain.

Moreover, relatively little is known regarding the brain mechanisms causing some children to gain excess weight, while others remain weight stable. In adolescents, some studies have investigated how differences in BOLD response predicted weight gain but results have varied. In adolescents with obesity, *increased* BOLD response in the striatum predicted weight gain at one-year later for one group (Yokum et al., 2014b) whilst this was not true in a different group of adolescents (Stice et al., 2013). In addition, a third study showed that *decreased* activation in the striatum was correlated with weight gain in adolescents one-year later (Stice et al., 2010). In the orbitofrontal cortex, both increased (Yokum et al., 2014b, 2011; Stice et al., 2015) and decreased (Stice et al., 2010) BOLD responses have predicted weight gain. In healthy weight adolescents, an elevated response in the prefrontal cortex and insula predicted weight

gain over a 3-year follow-up (Winter et al., 2017). Importantly, no research on neurobiological predictors has been conducted in children or adolescents under 15-years-old. Understanding how the brain plays a role in the prediction of weight gain in prepubescent children is imperative, as puberty is a critical time for weight gain (Kaplowitz, 2008).

To address these outstanding issues, the present study investigated how child body mass index (BMI) relates to neural circuitry across different modalities (e.g., structure and function) and multiple functional assessments (e.g., reward sensitivity, inhibitory control, working memory) in a large, racially and culturally diverse sample of 9-and-10-year-old children enrolled in the Adolescent Brain Cognitive Development Study (ABCD Study®). This study sought to use a cross-validated framework to: 1) identify brain correlates associated with BMI across several structural and functional modalities in children at 9-to-10-years-old; and 2) Determine if these brain modalities were predictive of weight gain at a one-year follow-up. Findings from these analyses may provide insight into the biomarkers associated with obesity from a disease perspective. Determining brain differences associated with BMI will be important for understanding the mechanisms underlying weight gain and, ultimately, for informing successful interventions.

2. Methods

2.1. Study design

Data for these analyses were obtained from the ABCD Study® study (Volkow et al., 2018) data version 2.0.1 (released, August 2019). The ABCD Study® is a 21-site, 10-year longitudinal investigation of cognitive development in U.S. children. In brief, 11,880 children were enrolled in the ABCD Study® at the ages of 9-and-10-years-old (between 2016–2018). Assessments are conducted in the laboratory each year while MRI is assessed every two years. Data presented in this paper include sMRI and fMRI, anthropometric, and demographic information from the baseline visit and anthropometric data from the one-year-follow-up. Currently, baseline data are available for the entire sample ($n = 11,875$), while year 1 (Y1) assessments have been released for 4915 children.

2.2. Exclusion criteria

Exclusion criteria for the ABCD Study® are documented elsewhere (Casey et al., 2018; Auchter et al., 2018; Garavan et al., 2018; Feldstein Ewing et al., 2018; Uban et al., 2018). In brief, children were ineligible if they had any MRI contraindications, like metal implants, not fluent in English, a history of major neurological disorders, prematurity at birth <28 weeks and/or hospitalization at birth >30 days. In addition, children were excluded from the present analyses for the following reasons: 1) underweight (according to the CDC age-sex-height-weight-specific cutoffs (Kuczmarski et al., 2000)); 2) had neurological, psychiatric or learning disabilities; 3) were taking medications known to affect food intake; 4) met diagnostic criteria for eating disorders (as assessed by the Kiddie Schedule for Affective Disorders and Schizophrenia [K-SADS]) (Kaufman et al., 1997); 5) mislabeled sex assigned at birth, incorrect sex-specific puberty questionnaire, or transgendered children; and 6) missing data for sex, puberty, age, race, or education. Because this study included MRI data, children were excluded from the analyses for the following MRI specific reasons: 1) failed FreeSurfer segmentation 2) excessive motion (volume scrubbing based on >0.2 mm framewise displacement for resting state fMRI (rsfMRI) and >0.9 mm for task fMRI), 3) < 200 degrees of freedom for each task fMRI and <12 min of rsfMRI data; 4) failed behavior performance on the task fMRI; 5) missing tabulated data. The Data Analysis, Informatics and Resource Center of the ABCD Study® was responsible for conducting all quality control, fMRI preprocessing, and calculation of behavioral performance. In addition, fMRI data collected using the Philips scanners was excluded

due to an error in preprocessing detected after the data were released.

2.2.1. Baseline sample

The sample size differed across MRI scans because not all children completed the entire MRI battery. The structural analyses contained the largest sample ($n = 6852$); fMRI analyses had smaller samples (rsfMRI $n = 4856$; Monetary Incentive Delay [MID] Task: $n = 4707$; Stop Signal Task (SST): $n = 4000$; Emotional n-Back [EN-back]: $n = 4453$) as performance rates differed across scans, and rsfMRI scans had stricter inclusion criteria (see [Tables 1 and 2](#) for demographics).

2.2.2. Y1 sample

At Y1, data were available for 4951 children but only 3422 passed the aforementioned exclusion criteria. In addition, to avoid including children who were dieting or had restrictive eating habits, children who lost weight from baseline to year one were excluded ($n = 70$). An additional 47 children were excluded due to measurement error (e.g., children were “taller” at baseline than Y1 by more than an inch). This left a final sample of 3052 children eligible for Y1 analyses (see [Table 3](#)).

2.2.3. Classification of child weight stability at Y1

All children and adolescents gain some weight throughout development, regardless if they are healthy weight or have obesity. However, extreme weight gain in a short period of time poses great health consequences ([Attard et al., 2013](#)) and may be early signs of preclinical eating disorders, such as binge eating. In this sample, children were free from eating disorders, yet a substantial number of children gained weight beyond normative development (see [Fig. 1A](#)). Therefore, we were interested in understanding if there were underlying brain associations between children with excessive (i.e., pathological) weight gain beyond normative development versus those who would remain weight stable (i.e., children who had normal developmental weight gain). Understanding differences in the brain between these groups may provide insight into the neurobiology associated with preclinical eating disorders, which are not detectable via diagnostic methods. Intervention programs targeting pathological overeating may also benefit from understanding what brain regions and functions relate to excessive weight gain. Therefore, to study the neural correlates of extreme weight gain,

Table 1

The number of children included for each modality after exclusion criteria were applied. BMI = body mass index; QC = Quality control; Structure = included cortical thickness, surface area, subcortical volume, Diffusion Tensor Imaging (DTI) which included fractional anisotropy (FA) and mean diffusivity (MD); w = weighted; FD = framewise displacement; ROI = Region of interest; SST = Stop Signal Task

Description	n				
Released data	11,875				
BMI percentile >5	11,393				
No reported medications known to affect food intake	10,620				
No reported neurological, psychological or learning disabilities	9504				
No reported eating disorders	8808				
Correct sex information/ not transgender	8717				
Complete info for sex, age, puberty, race, and education	8375				
Passed Freesurfer QC	7843				
Acceptable T1w image	7796				
	Structure	RS	MID	SST	EN-back
Acceptable T2w image	7456	–	–	–	–
Passed DTI QC	7254	–	–	–	–
Two runs that passed QC	–	7535	6251	6194	6150
Data without Philips scans	–	6523	5460	5392	5369
Resting state data >12 min	–	4873	–	–	–
FD < 0.9 mm	–	–	5317	5172	5127
Degrees of freedom >200	–	–	4990	4810	4760
Trials included >50	–	–	4976	–	–
Passed performance QC	–	–	4719	4437	4467
Available ROI tabulated data	6852	4856	4707	4225	4453
SST performance pass	–	–	–	4000	–

children were categorized into two groups: Weight Stable (WS) vs. Weight Gain (WG). WS and WG was defined using a previously published method: BMI z-score standard deviation (SD) change scores were calculated between two time points where WS was defined as a BMI z-score SD between $-0.2-0.2$, while weight gain was defined as ≥ 0.2 ([Geserick et al., 2018](#)), but we expanded upon this criterion. Thus, WS was defined as having a BMI z-score standard deviation (SD) between $-0.2-0.2$ ([Geserick et al., 2018](#)) and a BMI percentile $<70\%$ at both baseline and Y1. WG was defined as having a BMI z-score SD ≥ 0.2 and weight gain of >20 pounds within one year (i.e., > 1.0 SD above the mean weight gain for all children (see [Table 4](#))). Of note, children who lost weight between baseline and year one were not included in these analyses in order to avoid children who may be dieting or have restrictive eating. We chose to define two groups for the analyses rather than include everyone using BMI change score for several reasons. First, we were interested in evaluating the relationship between the brain and weight gain beyond normative development. Noting that some weight gain is typical at this age (see [Fig. 1A](#)) we did not want to conflate excessive weight gain with normative weight gain. In children, excessive weight gain cut offs are not clearly defined so we based our threshold on a previous method (as described ([Geserick et al., 2018](#))) and added an arbitrary threshold of 20-pounds to capture children who gained more pounds than one standard deviation from the mean. Of note, the mean weight gain for this group was 26.9 (SD = 7.1; Range: 20.5–61.9 pounds). Additionally, BMI z-scores and percentiles were not be appropriate as we previously found that they are not adequately adjusting for age and sex within the ABCD sample ([Adise et al., 2020, Under Review](#)). Second, changes in BMI, especially at the high ends, lacked sensitivity for rapid extreme weight gain (see [Fig. 1B](#)). For example, the BMI change for a child with a baseline BMI of 30 who gained 20 pounds one year later would be small and would not reflect substantial weight gain (see [Fig. 1C](#)). Third, although BMI change score cutoffs are used to define pathological weight gain in adults, these cutoffs do not exist for children, and therefore, it is not known what change score would be indicative of pathological weight gain in children. For these reasons, BMI alone is not a sensitive measure for clinical utility for extreme weight gain.

2.3. Non-imaging measures

2.3.1. Anthropometric measurements

A trained researcher measured children’s height (to the nearest inch) and weight (to the nearest 0.1 pound) at baseline and Y1 in light clothing and stocking feet twice. The average was recorded. Height and weight were converted to BMI age-sex-weight-height-specific percentiles and z-scores according to the Center for Disease Control (CDC) guidelines ([Kuczmarski et al., 2000](#)).

2.3.2. Pubertal assessment

Children and parents reported puberty using the sex-specific pubertal developmental scale ([Fischl et al., 2002; Petersen et al., 1988](#)) at baseline and Y1. Parent and child reports were averaged. The scale ranged from 1 (prepubescent) to 5 (post puberty).

2.3.3. Demographic assessments

The child’s age, sex, and race/ethnicity were reported by the parent at the baseline assessment. The highest reported parental education was used as a proxy for socioeconomic status. There were 22 options for race, which were collapsed into five categories: White, Black, Asian, Hispanic, Mixed/Other. There were 29 categories for education, which was treated as a continuous variable.

2.3.4. Kiddy schedule for affective disorders and schizophrenia for school-age children (KSADS)

The KSADS is an interview style questionnaire that assesses several psychiatric disorders, including eating disorders, in children ([Kaufman](#)

Table 2

Demographic characteristics of children who were included in the baseline structural, resting state (rs) functional magnetic resonance imaging (fMRI) and task fMRI linear elastic net regression analyses. The means, standard deviation (SD) and the range or sample size and percent are presented below. BMI z-score and percentiles were calculated using the CDC standards for age-sex-weight-height-specific cut offs (Kuczmarski et al., 2000). BMI = Body Mass Index; Kg = kilograms; cm = centimeters; HS = High school; GED = Generalized Education Degree. EN-back = Emotional N-back; MID = monetary incentive delay; SST = stop signal task.

Variable	Structural MRI		rsfMRI		EN-back fMRI		MID		SST	
	Mean (SD)	Range	Mean (SD)	Range	Mean (SD)	Range	Mean SD	Range	Mean SD	Range
Age	119.1 (7.5)	107–132	119.5 (7.6)	107–132	119.5 (7.6)	107–132	119.3 (7.6)	107–132	119.4 (7.6)	107–132
Puberty	1.9 (0.8)	1–5	1.9 (0.8)	1–5	1.9 (0.8)	1–5	1.9 (0.8)	1–5	1.9 (0.8)	1–5
BMI	19.1 (4.0)	13.8 - 53.9	18.8 (3.8)	13.8 - 52.8	19.0 (3.9)	13.8 - 53.9	18.9 (3.9)	13.8 - 53.9	19.0 (3.9)	13.8–42.8
BMI z-score	0.6 (1.0)	-1.6 - 3.1	0.5 (1.0)	-1.6 - 3.1	0.5 (1.0)	-1.6 - 3.1	0.5 (1.0)	1.6 - 3.1	0.5 (1.0)	-1.6 - 2.8
BMI percentile	64.7 (28.0)	5 - 99.9	62.7 (28.0)	5.0–99.9	63.2 (28.2)	5.0–99.9	63.6 (28.2)	5.0–99.9	64.3 (28.3)	5.0–99.8
Weight (kg)	38.2 (10.3)	21.3–97.1	37.8 (9.9)	21.3 - 93.9	38.0 (10.1)	21.3–97.1	38.0 (10.2)	21.3 - 93.9	38.0 (10.1)	21.3–97.1
Height (cm)	140.8 (8.0)	88.1 - 177.8	141.0 (7.9)	93.0 - 177.8	140.9 (8.0)	93.0 - 167.0	140.8 (8.0)	93.0 - 172.7	140.9 (7.8)	96.5–167.0
	n	%	n	%	n	%	n	%	n	%
Sex										
Male	3358	49.0	2233	46.0	2100	47.2	2216	47.1	1864	46.6
Female	3493	51.0	2623	54.0	2353	52.8	2491	52.9	2136	53.4
Race										
White	3770	55.0	2718	56.0	2571	57.7	2638	56.0	2332	58.3
Black	844	12.3	593	12.2	473	10.6	534	11.3	431	10.8
Hispanic	1430	20.9	964	19.9	897	20.1	981	20.8	790	19.8
Asian	147	2.1	97	2.0	94	2.1	99	2.1	86	2.2
Other	660	9.6	484	10.0	418	9.4	455	9.7	361	9.1
Education										
<HS	282	4.1	162	3.3	122	2.7	1143	24.3	121	3.1
HS/GED	565	8.2	373	7.7	314	7.1	1295	27.5	298	7.5
Some college	1680	24.5	1198	24.7	1087	24.4	1750	37.2	941	23.5
Bachelor's Degree	1820	26.6	1331	27.4	1248	28	149	3.2	1114	27.9
Postgraduate	2504	36.5	1792	36.9	1682	37.8	370	7.9	1526	38.2

Table 3

The number of children included after applying exclusion criteria for each scan separately. BMI percentiles were calculated using the CDC standards for age-sex-weight-height-specific cut offs (Kuczmarski et al., 2000). BMI = body mass index; Y1 = Year 1; QC = Quality control; Structure = included cortical thickness, surface area, subcortical volume, Diffusion Tensor Imaging (DTI) which included fractional anisotropy (FA) and mean diffusivity (MD); FD = framewise displacement; ROI = Region of interest. fMRI = functional magnetic resonance imaging; rsfMRI = resting state functional magnetic resonance imaging; SST = Stop Signal Task.

Description	n				
Released data	4915				
Passed baseline inclusion	3422				
No measurement error	3375				
Y1 BMI percentile >5	3338				
Y1 No reported medications known to affect food intake	3300				
Y1 No reported neurological, psychological or learning disabilities	3300				
Y1 Correct sex info/ not transgender	3282				
Y1 Complete info for sex, age, puberty, race, and education	3243				
Passed Freesurfer QC	3085				
Acceptable T1 image	3052				
Met weight stable/gainer criteria	1034				
	Structure	rsfMRI	MID	SST	EN-back
Acceptable T2 image	1002	–	–	–	–
Passed DTI QC	970	–	–	–	–
Two fMRI scans that passed QC	–	994	822	810	806
Available data without Phillips scans	–	869	728	712	719
Resting state data >12 min	–	555	–	–	–
Framewise displacement <0.9 mm	–	–	720	697	690
Degrees of freedom >200	–	–	669	649	632
Included 100 time points	–	–	666	–	–
Passed performance QC	–	–	630	619	607
Available ROI tabulated data	809	420	545	528	521
SST performance pass				490	

et al., 1997). It generates 32 DSM child psychiatric diagnoses. It includes categories for present, remission, and lifetime diagnoses. The scores are labeled as 0 (absence of diagnosis) and 1 (definitive diagnosis).

2.4. Neuroimaging measures

2.4.1. Image acquisition and preprocessing

Details of the ABCD Study® recruitment strategy, procedures, and MRI data acquisition and analyses are documented elsewhere (Volkow et al., 2018). Data were collected from 29 3 T scanners across 22 sites but three sites (e.g., data from Phillips scanners) were excluded from analyses. Children underwent a T1- and T2-weighted MRI, diffusion tensor imaging (DTI), rsfMRI, and three task-based fMRI scans. The scanning parameters (Garavan et al., 2018), imaging processing and analytics (Casey et al., 2018) and details describing each task are detailed elsewhere (Hagler et al., 2018). Data were parcellated with FreeSurfer using the Destrieux atlas (Casey et al., 2018), which contained 148 bilateral cortical regions of interest (ROIs). Fourteen bilateral subcortical ROIs were parcellated using FreeSurfer's subcortical segmentation (Destrieux et al., 2010). ROI estimates (e.g., mean beta weight, total gray matter volume) were available from the tabulated National Institutes of Mental Health Data Archive (NDA). As a quality control and outlier detection step, the top and bottom 1% of the data for each ROI were winsorized before statistical analyses were conducted.

2.4.2. sMRI

Structural data consisted of cortical thickness (mean thickness per ROI), cortical surface area (total surface area per ROI), and subcortical volume (total gray matter volume).

2.4.3. DTI

DTI assesses water diffusion in biological tissue to assess microstructural changes in white matter architecture. From these data, fractional anisotropy (FA) and mean diffusivity (MD) are computed. The FA calculation is presumed to reflect directionality estimates of tissue

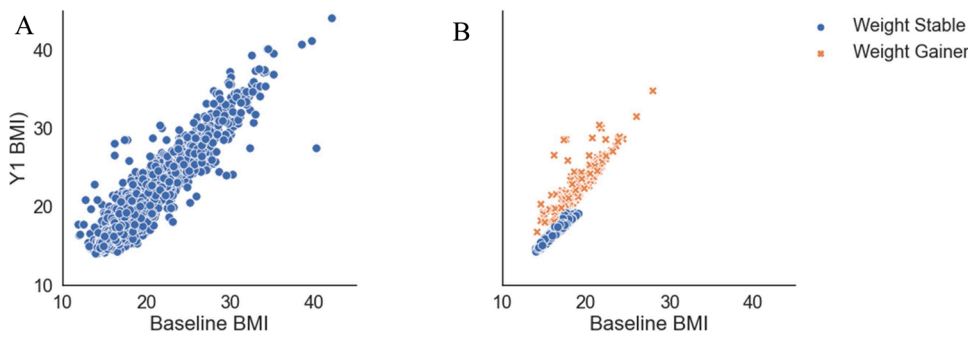


Fig. 1. Distributions of weight and BMI change. **A)** Weight change distribution in pounds from baseline line to year 1. The red bar indicates children who lost weight and were excluded. The dashed line indicates the mean. The yellow dashed line represents one standard deviation above the mean, where the yellow box highlights the number of children who gained more than 20 pounds. **B)** Baseline BMI plotted against Y1 BMI coded for all children and by weight stable and weight gain children. This figure highlights that the weight gain group was distributed across all levels of baseline BMI and that not all children met the criteria for weight stable or weight gainer. **C)** Examples of two participants'. (For interpretation of the references to colour in this figure legend, the reader is referred to the web version of this article).

Participant	B BMI	Y1 BMI	BMI Δ	B BMI%	Y1 BMI %	Weight (lbs) Δ
Par 1	25.78	26.31	0.53	98.09	97.71	27.35
Par 2	30.30	30.82	0.53	99.19	98.96	24.00

Table 4

Demographic characteristics of children who were included in the weight stable (WS) vs. weight gain (WG) logistic elastic net regression analyses. Means (m) and standard deviations (SD), or sample size and percent are presented below. WS criteria: Healthy weight at baseline and follow up and below the 70th BMI percentile, and a change in BMI z-score SD of < 0.2 . WG criteria: a change in body mass index (BMI) z-score SD $> 0.2 + 20$ pounds weight gain at follow up. BMI z-score and percentiles were calculated using the CDC standards for age-sex-weight-height-specific cut offs (Kuczmarski et al., 2000). Y1 = year 1; HS = high school; GED = Generalized Education Degree. BA = Bachelor's degree.

	WS (n = 637)	WG (n = 172)	p
Age (in months)			
Baseline (m, SD)	119.4 (7.5)	121.2 (7.0)	0.003
Y1	131.4 (7.7)	133.8 (7.0)	< 0.001
Puberty (m, SD)			
Baseline	1.7 (0.6)	2.1 (0.7)	< 0.001
Y1	1.9 (0.7)	2.6 (0.9)	< 0.001
BMI (m, SD)			
Baseline BMI	16.3 (1.0)	19.0 (2.2)	< 0.001
Y1 BMI	16.7 (1.1)	22.6 (2.8)	< 0.001
Baseline weight group (n, %)			
Healthy weight	637 (100.0)	117 (68.0)	< 0.001
Obese		10 (5.8)	
Overweight		45 (26.2)	
Y1 weight group (n, %)			
Healthy weight	637 (100.0)	49 (28.3)	< 0.001
Obese		50 (28.9)	
Overweight		74 (42.8)	
Sex (n, %)			
Male	293 (46.0)	97 (56.4)	0.020
Female	344 (54.0)	75 (43.6)	
Race (n, %)			
White	452 (71.0)	94 (54.7)	< 0.001
Black	30 (4.7)	21 (12.2)	
Hispanic	81 (12.7)	32 (18.6)	
Asian	19 (3.0)	1 (0.6)	
Other	55 (8.6)	24 (14.0)	
Parent Education (n, %)			
$< HS$	9 (1.4)	14 (8.1)	< 0.001
HS/GED	23 (3.6)	19 (11.0)	
Some college	124 (19.5)	50 (29.1)	
BA degree	183 (28.7)	38 (22.1)	
Postgraduate degree	298 (46.8)	51 (29.7)	

characteristics like myelination, fiber density etc. MD characterizes the diffusion magnitude and is related to the space between axons. The FA and MD estimates were calculated for the white matter sub-adjacent to each Destrieux ROI (Elman et al., 2017). DTI ROIs were used for the analyses presented in this paper because they were directly relatable to the cortical thickness and surface area ROIs. For completeness, the supplemental material contains analyses that included both DTI tracts and Destrieux labeled ROIs of sub-adjacent white matter estimates. Subcortical estimates for FA and MD were also calculated but are a mixture of both white and gray matter estimates.

2.5. fMRI paradigms

fMRI scans were acquired during performance of three behavioral tasks and at rest. The tasks are described below. Additional details are available in Supplemental Materials and are published elsewhere (Casey et al., 2018).

2.5.1. rsfMRI

Twenty minutes of resting state activity were collected. Resting state ROIs were parcellated using Gordon parcels (Gordon et al., 2016). Average time courses were calculated for each ROI. ROIs were grouped together according to the Gordon parcellated networks (e.g., default-mode network, fronto-parietal). Average pairwise ROI correlations were computed within and between each network. There were 91 cortical (78 inter- and 13 intra-network correlations) and 316 cortical to subcortical network correlations.

2.5.2. MID

The MID task assesses the BOLD response to anticipating and receiving monetary rewards and losses. Children pressed a button based on anticipation of either winning or losing two different sums of money. There were five anticipation conditions: small win \$0.50, large win \$5.00, small loss \$0.50, large loss \$5.00, \$0-no money (i.e., neutral) at stake and 10 outcome conditions (successes and fails on each of the five trial types). The following contrasts were analyzed: large reward vs. neutral anticipation, large loss vs. neutral anticipation, and positive vs. negative feedback for large reward and large loss trials. Additional information about this task can be found in the Supplemental Materials (S1.1.1).

2.5.3. SST

The SST task assesses inhibitory control. Children were encouraged to respond as quickly and accurately as they could to a GO stimulus and withhold responses to an infrequent STOP stimulus (presented 16.7 % of

the time). The following contrasts were analyzed: stop success (e.g., successful stop vs. successful go) and stop failure (e.g., unsuccessful stop vs. successful go). Additional information about this task can be found in the **Supplemental Materials (S1.1.2)**.

2.5.4. EN-back

The EN-back task assesses working memory and emotional processing. Children were shown a sequence of pictures (e.g., faces and places) and asked to determine if the current picture was the same (e.g., match, no match) as a target picture shown at the beginning of the block (0-back) or the same as the picture shown two pictures back in the sequence (2-back). The faces consisted of happy, angry and neutral faces. The following contrasts were analyzed: 2back vs. fixation, 0back vs. fixation and 2back vs. 0back. Additional information about this task can be found in the **Supplemental Materials (S1.1.3)**.

2.6. Analytic approach

2.6.1. Elastic-net regression

The entire sample was initially randomly partitioned into an 80 % training dataset for model building and 20 % testing dataset for model validation. Using the MATLAB package GLMnet (Qian et al., 2013), a five-fold, cross-validated elastic-net regression with a nested 20-fold cross-validation framework for hyperparameter tuning for alpha (α) and lambda (γ), was applied to the training set for feature selection. Generalizability was measured by applying the best fit model from the training set to the testing set. To assess the relationship between BMI at baseline and the brain, linear elastic-net regressions were conducted. Analyses used a raw BMI score, as the CDC BMI percentiles (Kuczmarski et al., 2000) were not adequately adjusting for age and sex in the ABCD Study® sample (Adise et al., 2020, Under Review). A logistic elastic-net regression was used to predict, with baseline MRI data, WS vs. WG at Y1. R^2 values are reported for the linear regressions and area under the curve (AUC) and p -values for the Y1 logistic prediction. Of note, ABCD Study® enrolled multiple sibling pairs including twins (Garavan et al., 2018). To ensure the independence of the test set from the training set, the best model fit was assessed on both the full test set and on the test set once all siblings were removed.

2.6.2. Modality inclusion criteria

Because covariates could potentially mask brain correlates of interest, a “brain-only” model was first developed for each modality of interest (i.e., separate elastic net regressions were run for structural data [DTI and FreeSurfer measures], rsfMRI, and each task fMRI dataset [$n_{\text{elastic net models}} = 5$]) to determine which modalities were related to BMI. In the brain-only analysis, for each modality, the variance explained on the test set was required to be at least 1% for that modality to be included in subsequent covariate analyses. For modalities that passed this threshold, their models were rerun with all the brain features from the significant modalities along with covariates of interest to quantify brain effects that persist in the presence of sociodemographic predictors. The covariates of interest (i.e., additional sociodemographic variables) included in the feature sets for the elastic net regressions were age, sex, puberty, race/ethnicity, parental highest education, handedness, and fMRI scanner ID. All of these covariates were available for feature selection, but the model included (selected) any covariates that improved the model performance (i.e., help explain variance). If the brain-only analysis produced a variance explained in the test set of $>1\%$, the elastic net regression was rerun with all features and covariates. Of note, prior to running the elastic net regression, dummy variables were created for all categorical variables.

2.6.3. Modality summary scores

In models that combined multiple MRI modalities or contrasts, beta weights from the elastic-net were converted to absolute values and summed to obtain an overall score per measurement type (e.g., FA,

cortical thickness, task activation). This was used for visualization purposes to determine which modality contributed most to the final elastic-net model.

2.6.4. Case matching, weight gain confirmatory analysis

Because the WS and WG groups differed in BMI at baseline, additional analyses were conducted to ensure that any successful model was predicting weight gain, and not discriminating the two groups based on their baseline weight differences. First, we relaxed the weight criterion for the WS group by including children who were over the 70th percentile at Y1. However, the WS group was still required to have a BMI SD change score between -0.2 and 0.2. Next, to identify WG and WS groups matched on baseline weight, a one-to-one matching for BMI at baseline was conducted using R’s MatchIt package (Ho, 2011) with the nearest neighbor method. This resulted in a new group of matched WS children ($WS_{\text{matched}(m)}$, $n = 172$) to be compared against the WG group ($n = 172$). We tested if the model from the WG prediction (unmatched for baseline BMI) correctly identified children in the WS_m group. If the original model was discriminating the groups on their current weight, rather than their weight gain, then we would expect it to erroneously identify WS_m children as weight gainers. However, if the model correctly identified children in the WS_m group as weight stable, this suggests the model is identifying brain regions associated with weight gain. For this analysis, the accuracy (percentage of WS_m children incorrectly identified as WG) is reported.

2.6.5. Comparing brain regions that classify current BMI and those that predict WS vs. WG

To investigate whether brain regions that classified baseline BMI were distinct from the brain regions associated with WS vs. WG at Y1, a logistic elastic-net regression was conducted predicting the Y1 WS vs. WG outcome but using only the brain features associated with BMI at baseline. Similarly, to quantify if the brain regions identified in the one-year prediction model also classified baseline BMI, the brain regions identified in the one-year prediction model were provided to a linear ridge regression explaining baseline weight. The ridge regression was forced to use the variables specified by each model but the beta weights were allowed to change.

3. Results

3.1. Brain modalities associated with BMI at baseline

As a first pass analysis to determine which modalities were associated with BMI, brain only models were run for each modality (e.g., structure, rsfMRI, and each of the three fMRI tasks). Brain structure, rsfMRI, and EN-back each explained more than 1% of the variance in BMI in the test set, while the MID and SST did not (see Table 5).

Table 5

The R^2 values (i.e., variance explained) for the training and test datasets for each brain modality. No covariates were added to the model to quantify the variance explained by the brain alone. The R^2 as well as the number of children in the analysis and features included are displayed per modality. MID = Monetary Incentive Delay Task; SST = Stop Signal Task; rsfMRI = resting state functional magnetic resonance imaging.

Modality	Training dataset		Testing dataset		# of brain features
	R^2	n	R^2	n	
Structure	0.27	5532	0.20	1319	396
rsfMRI	0.08	2739	0.05	653	166
MID	0.002	3787	0.0009	920	4
SST	0.03	3556	0.002	869	76
EN-back	0.04	3557	0.03	896	127

3.1.1. sMRI

To test whether BMI was related to brain structure, an elastic-net regression that included regional cortical thickness and surface area measures, subcortical volumes, DTI-based regional FA and MD, and sociodemographic variables was computed. The best model identified 313 structural ROIs, as well as sex, puberty, some races, education, handedness, and some scanners as features associated with BMI (see Fig. 2; for beta weights see Table S5 in the Supplemental Materials). Structural features consisted of 94 cortical thickness ROIs, 78 surface area ROIs, and the volumes of five subcortical ROIs. The best model also contained many sub-adjacent white matter measures that included FA from 58 cortical and seven subcortical ROIs, and MD from 66 cortical and five subcortical ROIs. In the training dataset, this explained 35 % of the variance in BMI, which generalized well to the test set (28 %; see Table 6). Removal of siblings from the test set produced similar results (27 %). Of note, intracranial volume (ICV) was a feature made available to the model but it was not selected. Moreover, as BMI was unrelated to total ICV, no additional corrections for ICV were conducted.

To understand the direction of the associations between the brain features and BMI, partial correlations, adjusted for the covariates of interest (e.g., sex, age, pubertal status, race, and education), showed that 64 % of the cortical thickness, surface area, FA and MD measures were negatively correlated with BMI. However, there were only positive partial correlations between BMI and subcortical gray matter volumes. These results indicate a widespread pattern of structural measures associated with BMI in 9-to-10-years-old.

3.1.2. rsfMRI

To test the relationship between BMI and rsfMRI, an elastic-net regression, including both Gordon parcellated network correlations and sociodemographic variables, was conducted. The best model identified 36 inter- and five intra-cortical network correlations, 107 cortical to subcortical inter-network correlations, as well as age, sex, puberty, some races, handedness, parental education and some scanners as features associated with BMI (for beta weights see Table S6 in the Supplemental Materials). The five intra-network correlations were from the default mode, frontoparietal, somatosensory hand, salience, and cingulo-opercular networks (see Fig. 3). Of note, the best model contained 45 % of all the cortical-to-cortical connections and 43 % of all the cortical-to-subcortical connections made available to the model. These rsfMRI features explained 21 % of the variance in BMI within the training set, but less variance explained in the test set (13 %) (see Table 6). Removal of siblings from the test set did not affect the variance

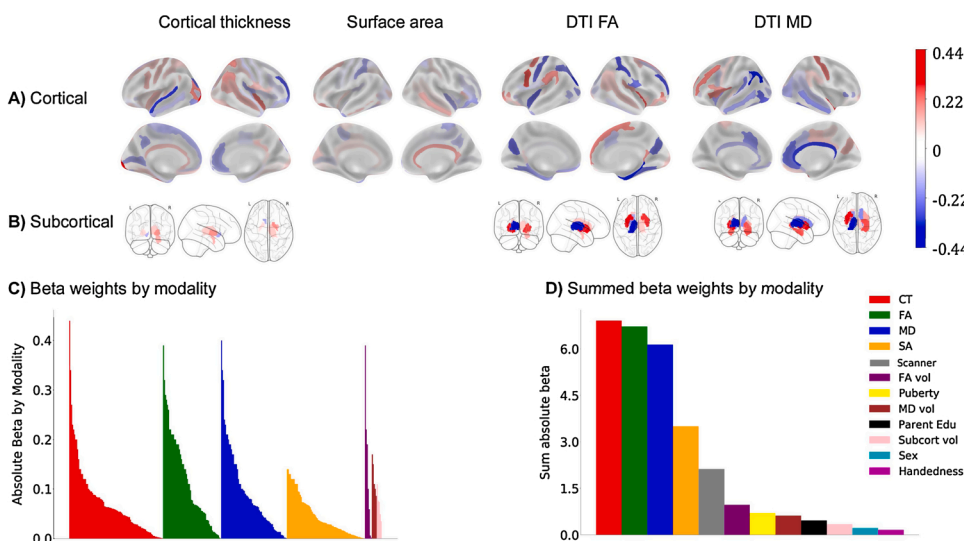


Fig. 2. Beta weights from the elastic net regression for each ROI and modality associated with BMI at baseline. **A)** Cortical ROIs; **B)** Subcortical ROIs. The signs of the beta weights are in reference to each other and do not necessarily represent thickening or thinning. However, 64 % of the structural ROIs identified were negatively correlated with BMI indicating that BMI was associated with smaller cortical thickness, surface area, and lower FA and MD (data not shown). Subcortically, BMI was positively correlated with gray matter volumes and most subcortical FA and MD white matter estimates (data not shown). **C)** Absolute beta weights sorted by each ROI and modality from the baseline elastic net model. **D)** Summed average absolute beta weights from the elastic net regression indicate magnitude of each contributing structural modality. CT = cortical thickness; DTI = Diffusion tensor imaging; FA = fractional anisotropy; MD = mean diffusivity; vol = volume; Subcort = subcortical; Edu = parent reported highest education.

explained (13 %). Partial correlations adjusted for the covariates of interest showed that 70 % of the rsfMRI measures had negative associations with BMI.

3.1.3. EN-back

To test the relationship between BMI and working memory, an elastic-net regression was conducted that included beta weight estimates per ROI for the 2-back, 0-back, and 2- vs 0-back contrasts from the EN-back task. The best model identified 13 EN-Back ROIs and several demographic variables including sex, puberty, some races, parent highest education, handedness, and some scanners as features associated with BMI. The model identified five ROIs from the 0-back task, seven ROIs from the 2-back task, and one ROI from the 2-back vs. 0-back contrast (see Fig. 4, see Table 7 for a list of ROIs). In the training set, these features explained 20.2 % of the variance in BMI and 15.7 % of the variance in BMI in the test set (see Table 6). Removal of siblings from the test set had a minor impact (16.4 %). Partial correlations adjusted for the covariates of interest showed BMI was associated with decreased activity in 62 % of the ROIs. However, there were no association between task performance (D' on either the 0-back, 2-back tasks, or the out of scanner memory recall test) and BMI.

3.1.4. MID

There was no association between BMI and the MID task ROIs.

3.1.5. SST

There was no association between BMI and the SST task ROIs.

3.2. Brain differences related to weight gain over a one-year period

3.2.1. Brain modalities that predictive disproportionate weight gain one year later

To determine which modalities were associated with predicting disproportionate weight gain one year later, brain only models were run for each modality (e.g., structure, rsfMRI, MID, SST, EN-back). Only baseline structural data predicted weight gain ($AUC_{\text{training}} = 0.71$, $p < 0.001$; $AUC_{\text{test}} = 0.61$, $p = 0.02$, features selected = 209; see Table 8).

3.2.2. sMRI

A logistic regression evaluated if sMRI at baseline predicted WS vs. WG one year later. The best model included 18 sMRI ROIs (see Table 9) as well as puberty at both baseline and Y1, parental highest education, four scanners, and intracranial volume ($AUC_{\text{train}} = 0.82$, $p = 6.1e-08$;

Table 6

The R^2 values (i.e., variance explained) for the training and test datasets for each brain modality. The R^2 as well as the number of children in the analysis and features included are displayed per modality; rsfMRI = resting state functional magnetic resonance. Covariate features for race, handedness and MRI scanner serial number were dummy coded.

Modality	Training dataset		Testing dataset		Removal of Siblings		# of brain features	# of covariate features
	R^2	n	R^2	n	R^2	n		
Structure	0.35	5532	0.27	1320	0.26	1089	365	32
rsfMRI	0.21	3918	0.13	938	0.13	938	148	16
EN-back	0.20	3557	0.16	896	0.16	775	29	27

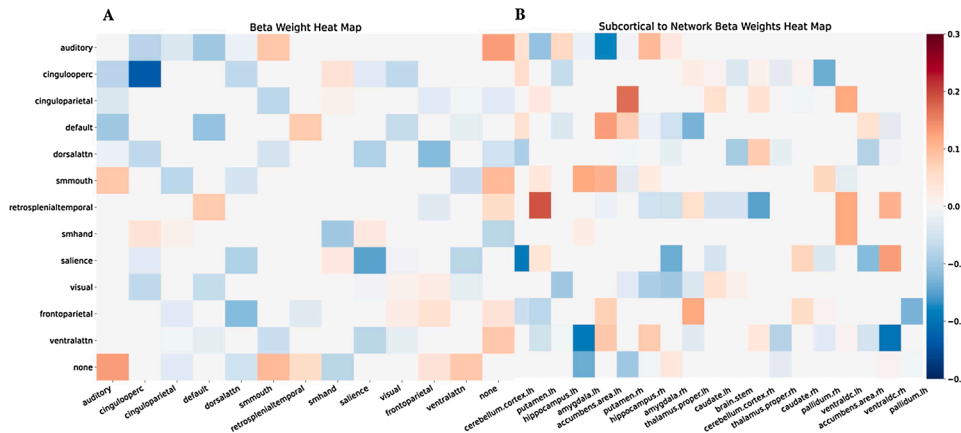


Fig. 3. Connectivity networks that are associated with BMI. The colour bar indicates beta weighting from the elastic net regression **A)** Cortical to cortical network correlations; **B)** Cortical to subcortical network correlations. Cingulooperc = cingulo-operculum; dorsalatn = dorsal attention; smmouth = somatosensory mouth; smhand = somatosensory hand; ventralatn = ventral attention; Rh = right hemisphere; Lh = left hemisphere; None = the none network are regions that did not fit into a classified network.

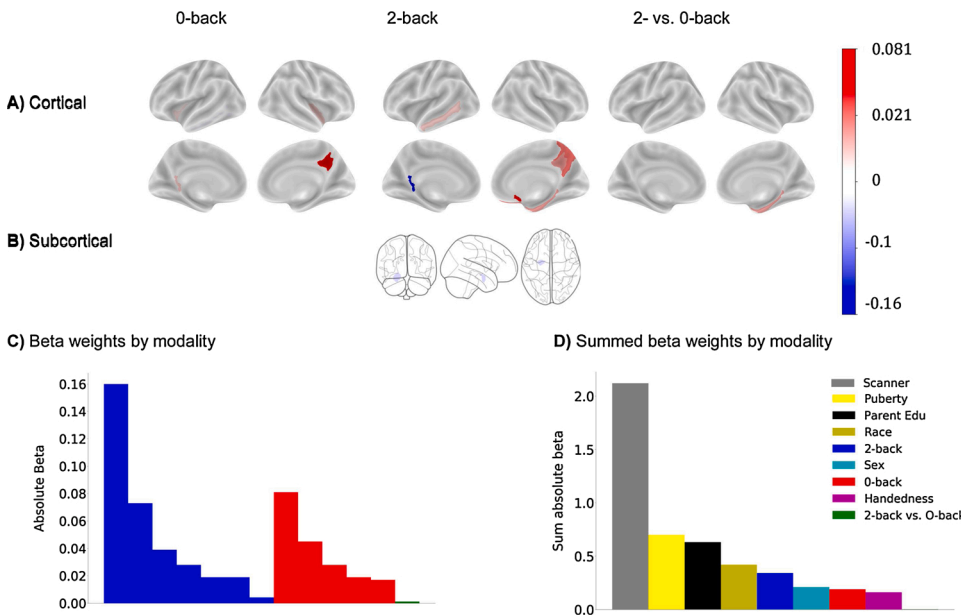


Fig. 4. Beta weights from the elastic net regression for each ROI for the EN-back predicting BMI at baseline. **A)** Cortical ROIs; **B)** Subcortical ROIs. The magnitudes of the beta weights are in reference to each other and do not necessarily represent increased or decreased activation, for example. **C)** Absolute beta weights sorted by each ROI and contrast from the baseline elastic net model. **D)** Summed average absolute beta weights from the elastic net regression to indicate magnitude of each contributing contrast. Edu = parent reported highest education.

$AUC_{test} = 0.78, p = 1.2e-07$). The structural ROIs consisted of five cortical thickness ROIs, and five surface area ROIs. The model contained sub-adjacent white matter measures that included FA from three cortical ROIs, and MD from four cortical and one subcortical ROI. Of note, removal of siblings had little impact on the results ($AUC = 0.77, p = 9.1e-07$, see Table 10; Fig. 5). In contrast to the baseline results, partial correlations adjusted for our covariates of interest showed that surface area, cortical thickness, and subcortical volume (in the pallidum) were positively associated with WG, while FA and MD estimates were negatively associated with WG.

3.2.3. Baseline BMI matching, weight gain confirmatory analysis

As previously noted, the WG and WS groups differed in baseline BMI. Therefore, we assessed if the prediction model was discriminating the children on their current weight difference. When applied to a sample of WS children (WS_m) who were matched to the WG group on baseline weight, only 3% were incorrectly identified as weight gainers. Because few children in the WS_m were misclassified as weight gainers, this suggests that the original model was not capitalizing on a difference in baseline BMI but identifying neural correlates of weight gain.

3.2.4. rsfMRI

rsfMRI at baseline did not predict WS vs. WG between baseline and

Table 7

The features selected by the elastic net regression for the EN-back. Region of interest (ROI) labels are in accordance with the Destrieux atlas labels. G = gyrus; S = sulcus; L = left; R = right.

ROI	Hemisphere	Beta
<i>0-back</i>		
G cingulate posterior ventral	L	-0.017
G insular short	L	-0.028
S circular insula inferior	R	-0.019
S subparietal	R	0.081
S temporal inferior	L	-0.045
<i>2-back</i>		
Amygdala	L	-0.039
G cingulate posterior ventral	L	-0.16
G precuneus	R	0.028
G subcallosal	R	0.073
G temporal middle	L	-0.019
S orbital medial olfactory	R	0.019
S subparietal	R	0.0042
<i>2-back vs. -0back</i>		
G occipital temporal medial parahippocampal	R	0.0012
<i>Covariate features</i>		
Female		0.21
Scanner 1		0.044
Highest Parent Education		-0.63
R handed		-0.016
White		-0.23
Black		0.12
Hispanic		0.07
Scanner 14		-0.0016
Scanner 16		0.16
Scanner 2		-0.059
Scanner 20		0.1
Scanner 24		0.069
Scanner 26		0.0062
Scanner 3		-0.22
Scanner 6		-0.051

Table 8

The area under the curve (AUC) for the training and test datasets for each brain modality from the logistic elastic net. No covariates were added to the model to quantify the probability of the AUC by the brain alone. The AUC and *p* values as well as the number of children in the analysis and features included are displayed per modality. WG = weight gain group; MID = Monetary Incentive Delay Task; SST = Stop Signal Task; rsfMRI = resting state functional magnetic resonance imaging.

Modality	Training dataset		Testing dataset		# of features
	AUC (<i>p</i>)	<i>n</i> _{Total} (<i>n</i> _{WG})	AUC (<i>p</i>)	<i>n</i> _{Total} (<i>n</i> _{WG})	
Structure	0.71 (0.0004)	652 (136)	0.61 (0.02)	157 (36)	209
rsfMRI	0.06 (0.06)	333 (70)	0.45 (0.25)	87 (13)	7
MID	0.5 (0.5)	430 (85)	0.5 (0.5)	115 (26)	2
SST	0.5 (0.5)	413 (80)	0.5 (0.5)	115 (27)	2
EN-back	0.5 (0.5)	410 (81)	0.5 (0.5)	111 (24)	-

Y1.

3.2.5. MID

MID activation at baseline did not predict WS vs. WG between baseline and Y1.

3.2.6. SST

SST activation at baseline did not predict WS vs. WG between baseline and Y1.

Table 9

The features selected by the logistic elastic net regression that predicted children who gained more than 20 pounds within a year. Region of interest (ROI) labels are in accordance with the Destrieux atlas labels. G = gyrus; S = sulcus; L = left; R = right; *ROIs that were also associated with baseline BMI, although the directionality differed.

ROI	Hemisphere	Beta
<i>Cortical thickness</i>		
G rectus*	L	-0.006
S collateral transverse posterior*	L	0.029
S intermedius primus (of Jensen)*	L	0.0057
S pericallosal*	L	0.0071
G and S fronto-marginal gyrus (of Wenicke)*	R	-0.071
<i>Surface Area</i>		
G occipital temporal medial parahippocampus	L	0.02
G temporal superior transverse*	L	0.00083
G parietal inferior angular	R	0.0013
S circular insula inferior*	R	0.071
S occipital anterior	R	-0.13
<i>DTI FA</i>		
G and S paracentral	L	-0.049
S orbital lateral*	L	0.074
S intraparietal and P transverse	R	-0.022
<i>DTI MD</i>		
G insula large and S central insula	L	-0.04
G and S cingulate anterior*	R	-0.047
G parietal superior*	R	0.054
G orbital medial olfactory	R	-0.017
<i>DTI MD Subcortical</i>		
Palladium	R	-0.038
Intercranial Volume		0.05
<i>Covariate features (non-brain)</i>		
Baseline puberty		0.18
Year 1 puberty		0.44
Highest parental education		-0.3
Scanner 2		-0.11
Scanner 5		0.00056
Scanner 16		0.14
Scanner 22		0.12

3.2.7. EN-back

EN-back at baseline did not predict WS vs. WG between baseline and Y1.

3.3. Investigating the relationship between brain regions that classify current BMI vs. those that predict WS vs. WG

3.3.1. Overlapping regions associated with BMI at baseline and WG at Y1

Ten out of the 19 structural brain regions that predicted WG by the one year follow up were also regions associated with baseline BMI. This included all five of the regions in which cortical thickness predicted WG (see Table 9). However, the direction of the effects differed for cortical thickness between the baseline BMI and WG analysis. For example, greater BMI at baseline was associated with thinner cortical thickness, whereas children in the WG group had thicker cortices at baseline regardless of their baseline BMI. Regarding the DTI data, only one out of three ROIs showing FA effects and two out of four ROIs showing MD effects were associated with both baseline BMI and weight gain. In addition, two out of the five surface area ROIs were associated with both baseline BMI and WG. The directionality of effects was the same as baseline for the DTI and surface area ROIs.

3.3.2. Baseline, Y1 model comparisons

When applying the prediction ROIs to the baseline sample, the features that predicted WG explained merely 9% of the variance in baseline BMI (compared to the 27 % explained by the baseline model).When

Table 10

The AUC and p value for the training and test dataset for the WG prediction analysis. The AUC as well as the number of children in the analysis and features included are displayed for the training and testing dataset for children included in the Y1 structural prediction analysis. Of note, covariates were dummy coded for race, sex, handedness, and MRI scanner serial number. The brain features included cortical thickness, surface area, diffusion tensor imaging (DTI) estimates of fractional anisotropy (FA) and mean diffusivity (MD), and subcortical volume regions. The beta weight for each brain feature is listed in Table 9. WG = weight gain; WS = weight stable; AUC = area under the curve.

Structure	Training dataset		Testing dataset		Removal of Siblings		# of brain features	# of covariate features
	AUC (p)	n_{Total} (n_{WG})	AUC (p)	n	AUC(p)	n_{Total} (n_{WG})		
WS vs. WG	0.82 (<0.0001)	652 (136)	0.78 (<0.0001)	157 (36)	0.77(<0.0001)	148 (34)	19	7

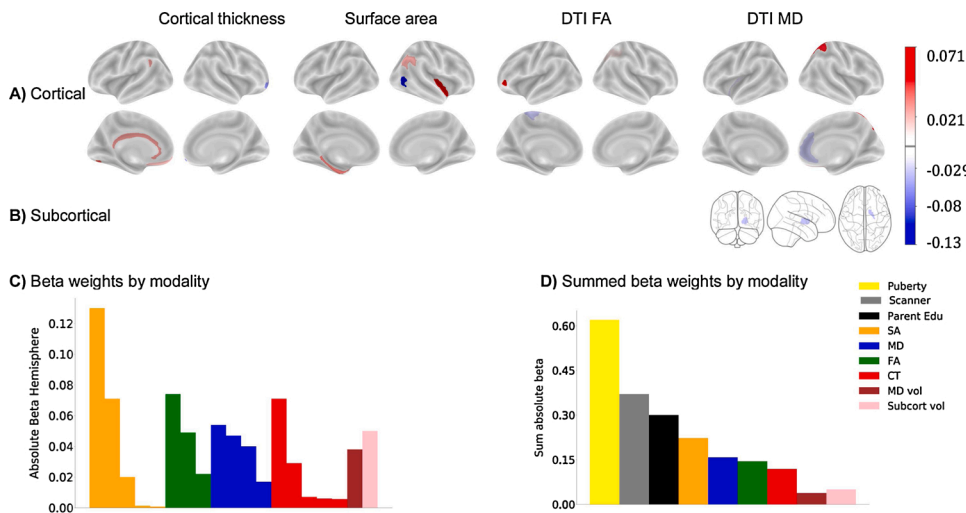


Fig. 5. Beta weights from the logistic elastic net regression for each ROI and structural modality predicting weight gain at the one year follow up. **A)** Cortical ROIs; **B)** Subcortical ROIs. The magnitudes of the beta weights are in reference to each other and do not necessarily represent thickening or thinning, for example. **C)** Absolute beta weights sorted by each ROI and modality from the weight gain at year 1 prediction elastic net model. **D)** Summed average absolute beta weights from the elastic net regression to indicate magnitude of each contributing structural modality. CT = cortical thickness; SA = Surface area; DTI = Diffusion tensor imaging; FA = Fractional anisotropy; MD = Mean diffusivity; vol = Volume. Edu = Parent highest reported education.

applying the baseline model to the WS vs WG sample, the model still identified children with WG, but the AUC in the test set (0.74) was lower than that observed with the best prediction model (0.79). This difference in AUC was not significant.

4. Discussion

Using a large and racially diverse group of 9-to-10-year-old children enrolled in the ABCD Study®, we shed light on the brain modalities associated with current BMI and those that predict weight gain one year later. Across several modalities, current BMI was associated with brain structure (i.e., regional measures of cortical thickness, surface area, subcortical volume, and FA and MD diffusion measures), functional rsfMRI connectivity and EN-back activations in select regions associated with working memory. Task-based functional activation on the MID (i.e., reward anticipation and outcome), and SST (i.e., motor response inhibition) did not show associations with BMI at ages 9-to-10-years-old. In addition, brain structure was predictive of children who would gain more than 20 pounds one year later. However, rsfMRI and task-based fMRI across the MID, SST, and EN-back were not.

Traditionally, brain-BMI associations have been investigated within a single modality. Yet, few studies have converged on a consistent set of findings. Obesity in children has been related to the cortical thinness of the frontal cortex (Alosco et al., 2014; Ronan et al., 2019; Carbine et al., 2019) and/or greater subcortical volumes of specific appetitive regions like the hippocampus (Mestre et al., 2017), pallidum (de Groot et al., 2017), amygdala and/or accumbens (Perlaki et al., 2018; Rapuano et al., 2017). In our study, BMI showed global (i.e., widespread) associations within multiple modalities (e.g., cortical thickness, surface area). BMI at 9-to-10-years-old was associated with thinner cortices (as previously reported (Laurent et al., 2019)), but also to reduced surface area, larger subcortical volumes and smaller FA and MD estimates. Together, cortical thickness, surface area, subcortical volume, and DTI estimates of white matter, explained between 27 % of the variance in current BMI

within the test set. Our findings differ slightly from the literature but no studies (besides ours) have collected multiple modalities and related them to BMI within the same subject. Evaluating multiple within subject measures allows for a comprehensive picture, as it captures the variance explained by each modality and their relative value in respect to each other. In addition, the large sample size of the ABCD Study® allowed us to capture the variance explained in BMI above and beyond the contribution of sociodemographic factors, which may have confounded results from smaller studies (Garavan et al., 2018).

From a disease perspective, the association between BMI and differences in gray and white matter may be indicative of neuroinflammation (Ho et al., 2010), an early consequence of obesity (Mendes et al., 2018; Guillemot-Legrís and Muccioli, 2017). Neuroinflammation is thought to occur in response to repeated intake of high fat foods, as the hypothalamus triggers inflammatory responses in reaction to intake of free fatty acids found in fatty foods; overconsumption of high fat foods is a risk factor for childhood obesity (Arango-Angarita et al., 2018). Through this proposed mechanism, overexpression of pro-inflammatory markers impairs synaptic plasticity, neurogenesis and neuromodulation (Mendes et al., 2018). Although hypothalamic volume was not selected as an association of BMI, our analysis does not rule out that overexpression of pro-inflammatory and appetitive hormones in this region may relate to structural differences observed elsewhere in the brain. Thus, neuroinflammation may explain why brain structure (e.g., gray and white matter) was related to BMI in children, specifically at baseline. It is important to note, that although our data align with the theory of neuroinflammation, our analyses cannot determine causal mechanisms. So, although obesity is associated with neuroinflammation (Mendes et al., 2018; Guillemot-Legrís and Muccioli, 2017), it is not known if structural variation existed prior to obesity onset and causes overeating (i.e., biological cause) or if gray and white matter alterations are solely consequences of overeating/obesity onset. However, the relative strength of association between each modality and BMI (i.e., the comparison of the summed absolute beta weights for each modality;

Fig. 2) showed that gray matter features (e.g., cortical thickness) contributed more to the model, than white matter features (e.g., DTI FA and MD). One reason for this may be that white matter may restructure in response to gray matter alterations (Radetz et al., 2020). Because these children were relatively young (9-to-10-years-old), future research will provide insights into how gray and white matter change in response to weight gain over time during a critical developmental period.

The prefrontal cortex, which is associated with inhibitory control (Aron et al., 2014) (e.g., dorsolateral prefrontal cortex) and reward processing (e.g., ventromedial and medial prefrontal cortex) emerged as an area with substantial structural associations with BMI. The literature suggests that altered structure and processing in regions associated with inhibitory control and reward processing may drive overeating (Kroemer and Small, 2016) due to an imbalance in function between these regions. For example, the theory proposes that altered response to food in regions associated with reward coupled with an altered response in regions associated with inhibitory control (i.e., inability to stop behavior) leads to food intake. Our sMRI findings are consistent with this theory as BMI was negatively correlated with brain structure in both regions associated with reward and inhibitory control. These regions have been proposed to be direct drivers of food intake due to their involvement in liking (e.g., the hedonics associated with pleasure of a reward) and wanting (e.g., the motivational drive to obtain a reward) mechanisms (Berridge et al., 2010). Additionally, studies have shown that greater BOLD response to food compared to money rewards in these regions was related to overeating in two different laboratory test meals (Adise et al., 2018). Thus, one interpretation of our results is that larger subcortical volumes in regions associated with regulating food intake and reward may contribute to overactive appetitive drives (i.e., overeating), and hence, weight gain. However, because ABCD did not collect objective measures of food intake, this should be further investigated in future studies.

The structural findings indicated that several regions involved in reward processing and inhibitory control were related to current BMI and WG at Y1 but task-based fMRI reward and inhibitory control processes (as assessed by the MID and SST) were not. This was striking because many studies show associations between fMRI in key regions associated with reward and inhibitory control in adults and children (Yokum et al., 2014a; Bohon, 2017; Batterink et al., 2010; Bruce et al., 2010; Davids et al., 2010; Bruce et al., 2013; Van et al., 2016; Boutelle et al., 2015; Rolls, 2011; Frank et al., 2013; Avery et al., 2017). Of relevance, our study used active, cognitively demanding decision-making tasks in the absence of food rewards, which is in contrast to those that used food-based passive viewing tasks. Food-based passive viewing tasks provide limited insight into actual psychological mechanisms because they lack cognitive demands and may be ineffective for assessing neural processing deficits in children. In addition, the MID and SST assess specific types of reward (e.g., anticipation and feedback of monetary rewards) and inhibitory control (e.g., prepotent motor inhibition) processes, which may not be optimal for exposing deficits in the context of food decision-making and obesity. However, it is also plausible that task-fMRI (whether it is passive-viewing tasks or active-tasks) may be better for understanding the neurological mechanisms associated with the behavioral phenotype of overeating (a risk factor for obesity) rather than classifying actual BMI (a consequence of overeating). Lastly, because reward and inhibitory control processes are undergoing maturation during adolescence (Shulman et al., 2016), functional relationships with BMI may be observed later in development. As these children continue to age, ABCD Study® will provide insight into how structural and functional relate to BMI over time.

The only fMRI task associated with BMI was the EN-back working memory task. When specifically looking at the working memory contrast (e.g., 2- vs. 0-back), activation in the parahippocampal gyrus was the only region associated with BMI. This result converges with previous findings in a similar cohort of children with higher BMI showing that thinner cortices in this region relate to performance on executive

functioning assessment such as card and list sorting and matrix reasoning (Laurent et al., 2019), which are assessments of working memory. Additionally, structural variation in this region was associated with higher BMI and weight gain prediction at Y1. The literature investigating appetitive hormones and brain function are relevant for understanding possible links between obesity and structural changes in regions associated with working memory. Appetitive hormones (e.g., ghrelin, insulin) activate hippocampal regions (Miller et al., 2014) and in both animal and human studies, dysregulation of these hormones (due to overeating) have been associated with memory impairment. This suggests that structural differences in working memory regions may occur due to overexpression of hunger regulatory and/or pro-inflammatory hormones that are more pronounced with obesity. However, because ABCD did not collect measurements of appetitive hormones, future studies are needed to explore this relationship further. Of note, although the EN-back task assesses working memory, it also contained an emotional component. Emotion reactivity can interfere with working memory processes, which makes it difficult to generalize these findings to working memory a part from the emotional component. Therefore, future studies should investigate the correlations between BMI and activation on working memory tasks without an emotional component

In line with structural findings, rsfMRI revealed widespread functional connectivity associations with BMI. The relatively few rsfMRI studies conducted in children and adolescents showed that BMI was associated with greater connectivity between frontal regions, such as the left middle frontal gyrus and the left ventromedial prefrontal cortex and left lateral orbitofrontal cortex (Black et al., 2014). Although one study showed connectivity between the insula and anterior cingulate cortex (i.e., cingulo-parietal network) (Moreno-Lopez et al., 2016) was related to childhood obesity in children, the directional effect (i.e., decreased connectivity) was opposite to our findings (i.e., increased connectivity). Thus, one interpretation could be that altered connectivity between cognitive control and reward regions may be one reason for overeating. This theory is deeply rooted in that of the Reflective-Impulsive Dual Mechanisms model (Hofmann, 2008), which proposes that behavioral responses to rewarding stimuli are driven by the balance between reward and inhibitory control processes. This theory proposes that when overeating occurs when inhibitory control processes are not able to suppress behavioral responses to rewarding stimuli. However, because ABCD did not collect measures of food intake, this hypothesis needs to be evaluated with future studies. Further, as baseline BMI was related to connectivity of dorsal and ventral attention, default mode, auditory, visual and somatosensory networks, the relationship between obesity and resting state activity appears more widespread and complex. Future studies should investigate how these networks relate to objective overeating.

sMRI measures, including surface area, cortical thickness, and sub-adjacent DTI estimates of FA and MD, and subcortical estimates of MD were the only brain modalities associated with WG. Although there was some overlap with the regions that classified baseline BMI, distinct regions within surface area (e.g., parahippocampal gyrus, inferior parietal gyrus, anterior occipital sulcus), and sub-adjacent white matter FA (e.g., paracentral gyrus, intraparietal sulcus) and MD measures (e.g., insula, orbital medial olfactory gyrus) predicted WG at Y1. These findings suggest the brain may show structural variation prior to WG particularly in regions known to be associated with food intake, like the parahippocampal gyrus (Brooks et al., 2013) and insula (Rolls, 2015). One interpretation of these results is that altered white matter architecture and smaller surface areas in regions associated with food intake, may be related to phenotypic overeating and suggest a potential mechanism leading to rapid weight gain.

Children who were in the Y1 WG group varied in weight status at baseline (i.e., healthy weight, overweight or obese (Kuczmarski et al., 2000)). This is important because as these results could potentially identify children who are more likely to transition from healthy weight

into overweight/obese, meaning that children who are not WS could be readily identified. Rapid weight gain is a concern because it increases the risk for cardiovascular disease later in life (Attard et al., 2013), and subclinical cardiovascular risks can be apparent as early as young adulthood (Hao et al., 2018). As there are significant health consequences of WG, particularly in children (Attard et al., 2013), understanding the neurological associations that are predictive of WS vs. WG may provide valuable insight for understanding and improving the health outcomes for these children. However, future research is needed to examine how these brain regions relate to objective overeating and how they change in response to weight gain over time.

4.1. Strengths and limitations

The data presented in this paper contribute to the literature by identifying generalizable structural and functional brain measures related to current BMI and future weight gain in the largest-to-date, racially and culturally diverse group of children age 9-to-10-years-old. We highlight the potential utility of MRI to identify children who are at higher risk for obesity. Because childhood obesity is associated with various early-onset medical consequences (Reilly et al., 2003) as well as fiscal implications (Finkelstein et al., 2009), improved risk assessment has potential benefits for child health and public policy.

We note several limitations. The ABCD Study® did not collect assessments of objectively measured food intake. Therefore, these findings do not offer insight into whether differences in brain structure are related to disordered eating. The ABCD Study® did not collect parent height and weight, which limits our ability to explore hereditary influences related to weight gain. Although heritability can be studied via twin designs, this information would only provide heritability estimates for sibling pairs and not to singletons within the study. However, a future direction is to investigate the role of heritability and extreme weight gain. Similarly, the ABCD Study® did not collect inflammatory biomarkers at baseline which limits an examination of how neuro-inflammation relates to brain structure and function in children. The neuroimaging data were cross-sectional, which provides limited insight into temporal changes in the brain associated with WG. However, future releases of the ABCD Study®, which will include longitudinal within-subject neuroimaging data will address this limitation.

5. Conclusion

Obesity rates are increasing with sparse understanding of the neurological basis driving weight gain. Using a large sample and cross-validated analytic approach we identified reliable associations of current BMI in a large and racially diverse group of 9-to-10-year-old children. BMI was associated with widespread structural differences, altered rsfMRI, and working memory during the EN-back task. Of most interest, our findings identified specific brain regions predictive of rapid weight gain one year later. Rapid weight gain poses detrimental health consequences, and may be a sign of disordered eating. Thus, these results have direct implications for intervention programs.

Data statement

The data used in this manuscript is available through the National Data Archives Database.

Funding

Data used in the preparation of this article were obtained from the Adolescent Brain Cognitive Development Study (ABCD Study®) (<https://abcdstudy.org>), held in the NIMH Data Archive (NDA). This is a multisite, longitudinal study designed to recruit more than 10,000 children age 9–10 and follow them over 10 years into early adulthood. The ABCD Study is supported by the National Institutes of Health and

additional federal partners under award numbers U01DA041048, U01DA050989, U01DA051016, U01DA041022, U01DA051018, U01DA051037, U01DA050987, U01DA041174, U01DA041106, U01DA041117, U01DA041028, U01DA041134, U01DA050988, U01DA051039, U01DA041156, U01DA041025, U01DA041120, U01DA051038, U01DA041148, U01DA041093, U01DA041089, U24DA041123, U24DA041147. A full list of supporters is available at <https://abcdstudy.org/federal-partners.html>. A listing of participating sites and a complete listing of the study investigators can be found at https://abcdstudy.org/consortium_members/. The ABCD Study® consortium investigators designed and implemented the study and/or provided data but did not necessarily participate in analysis or writing of this report. This manuscript reflects the views of the authors and may not reflect the opinions or views of the NIH or the ABCD Study® consortium investigators. The study was also funded by the Tobacco Center of Research Science (TCORS) Training Grant under award number U54DA036114 from the National Institute on Drug Abuse and Food and Drug Administration (FDA); 3) The National Institute on Drug Abuse of the National Institutes of Health under award number T32DA043593; 4) The National Institute of General Medical Science COBRA grant under award number P20GM103644. The content is solely the responsibility of the authors and does not necessarily represent the official views of the NIH, ABCD Study®, or TCORS.

Declaration of Competing Interest

The authors declare that they have no known competing financial interests or personal relationships that could have appeared to influence the work reported in this paper.

Acknowledgements

The authors' responsibilities were as follows – SA wrote the manuscript and performed the analysis with the guidance of NA, MO, SH, DK, SM, AP, and HG. SA, SM, BC, JL, AP, and HG. SA conceptualized and curated the data with the guidance of HG. HG and AP provided funding for the project as part of the ABCD Study® consortium. All authors contributed feedback, and read, and approved the final manuscript. No authors report any conflicts of interest. The ABCD Study® consortium investigators designed and implemented the study and/or provided data but did not necessarily participate in analysis or writing of this report.

Appendix A. Supplementary data

Supplementary material related to this article can be found, in the online version, at doi:[10.1016/j.dcn.2021.100948](https://doi.org/10.1016/j.dcn.2021.100948).

References

- Adise, S., Geier, C.F., Roberts, N.J., White, C.N., Keller, K.L., 2018. Is brain response to food rewards related to overeating? A test of the reward surfeit model of overeating in children. *Appetite* 128 (June), 167–179. <https://doi.org/10.1016/j.appet.2018.06.014>.
- Adise, S., Geier, C.F., Roberts, N.J., White, C.N., Keller, K.L., 2019. Food or money? Children's brains respond differently to rewards regardless of weight status. *Pediatr. Obes.* 14 (2), e12469 <https://doi.org/10.1111/ijpo.12469>.
- Alosco, M.L., Stanek, K.M., Galisto, R., et al., 2014. Body mass index and brain structure in healthy children and adolescents. *Int. J. Neurosci.* 124 (1), 49–55. <https://doi.org/10.3109/00207454.2013.817408>.
- Arango-Angarita, A., Rodríguez-Ramírez, S., Serra-Majem, L., Shamah-Levy, T., 2018. Dietary energy density and its association with overweight or obesity in adolescents: a systematic review of observational studies. *Nutrients* 10 (11). <https://doi.org/10.3390/nu10111612>.
- Aron, A.R., Robbins, T.W., Poldrack, R.A., 2014. Inhibition and the right inferior frontal cortex: one decade on. *Trends Cogn. Sci.* 18 (4), 177–185. <https://doi.org/10.1016/j.tics.2013.12.003>.
- Attard, S.M., Herring, A.H., Howard, A.G., Gordon-Larsen, P., 2013. Longitudinal trajectories of BMI and cardiovascular disease risk: the national longitudinal study of adolescent health. *Obesity* 21 (11), 2180–2188. <https://doi.org/10.1002/oby.20569>.

- Auchter, A.M., Hernandez, M., Heyser, C.J., et al., 2018. Developmental Cognitive Neuroscience A description of the ABCD organizational structure and communication framework. *Dev. Cogn. Neurosci.* 32 (April), 8–15. <https://doi.org/10.1016/j.dcn.2018.04.003>.
- Avery, J.A., Powell, J.N., Breslin, F.J., et al., 2017. Obesity is associated with altered mid-insula functional connectivity to limbic regions underlying appetitive responses to foods. *J. Psychopharmacol. (Oxford)* 31 (11), 1475–1484. <https://doi.org/10.1177/0269881117728429>.
- Batterink, L., Yokum, S., Stice, E., 2010. Body mass correlates inversely with inhibitory control in response to food among adolescent girls: an fMRI study. *Neuroimage* 52 (4), 1696–1703. <https://doi.org/10.1016/j.neuroimage.2010.05.059>.
- Berridge, K.C., Ho, C.-Y., Richard, J.M., DiFeliceantonio, A.G., 2010. The tempted brain eats: pleasure and desire circuits in obesity and eating disorders. *Brain Res.* 1350, 43–64. <https://doi.org/10.1016/j.brainres.2010.04.003>.
- Berthoud, H.-R., Münzberg, H., Richards, B.K., Morrison, C.D., 2012. Neural and metabolic regulation of macronutrient intake and selection. *Proc. Nutr. Soc.* 71 (03), 390–400. <https://doi.org/10.1017/S0029665112000559>.
- Black, W.R., Lepping, R.J., Bruce, A.S., et al., 2014. Tonic hyper-connectivity of reward neurocircuitry in obese children. *Obesity* 22 (7), 1590–1593. <https://doi.org/10.1002/oby.20741>.
- Bohon, C., 2017. Brain response to taste in overweight children: a pilot feasibility study. *Lu L, ed. PLoS One* 12 (2), 1–9. <https://doi.org/10.1371/journal.pone.0172604>.
- Boutelle, K.N., Wierenga, C.E., Bischoff-Grethe, A., et al., 2015. Increased brain response to appetitive tastes in the insula and amygdala in obese compared with healthy weight children when sated. *Int. J. Obes.* 39 (4), 620–628. <https://doi.org/10.1038/ijo.2014.206>.
- Brooks, S.J., Cedernaes, J., Schiöth, H.B., 2013. Increased prefrontal and parahippocampal activation with reduced dorsolateral prefrontal and insular cortex activation to food images in obesity: a meta-analysis of fMRI studies. *PLoS One* 8 (4). <https://doi.org/10.1371/journal.pone.0060393>.
- Bruce, A.S., Holsen, L.M., Chambers, R.J., et al., 2010. Obese children show hyperactivation to food pictures in brain networks linked to motivation, reward and cognitive control. *Int. J. Obes.* 34 (10), 1494–1500. <https://doi.org/10.1038/ijo.2010.84>.
- Bruce, A.S., Lepping, R.J., Bruce, J.M., et al., 2013. Brain responses to food logos in obese and healthy weight children. *J. Pediatr.* 162 (4), 759–764. <https://doi.org/10.1016/j.jpeds.2012.10.003> e2.
- Burger, K.S., Berner, L.A., 2014. A functional neuroimaging review of obesity, appetitive hormones and ingestive behavior. *Physiol. Behav.* 136, 121–127. <https://doi.org/10.1016/j.physbeh.2014.04.025>.
- Carbine, K.A., Duraccio, K.M., Hedges-Muncy, A., Barnett, K.A., Kirwan, C.B., Jensen, C. D., 2019. White matter integrity disparities between normal-weight and overweight/obese adolescents: an automated fiber quantification tractography study. *Brain Imaging Behav.* <https://doi.org/10.1007/s11682-019-00036-4>. February.
- Casey, B.J., Cannonier, T., Conley, M.I., et al., 2018. The adolescent brain cognitive development (ABCD) study: imaging acquisition across 21 sites. *Dev. Cogn. Neurosci.* 32 (January), 43–54. <https://doi.org/10.1016/j.dcn.2018.03.001>.
- Davids, S., Lauffer, H., Thoms, K., et al., 2010. Increased dorsolateral prefrontal cortex activation in obese children during observation of food stimuli. *Int. J. Obes.* 34 (1), 94–104. <https://doi.org/10.1038/ijo.2009.193>.
- de Groot, C.J., van den Akker, E.L.T., Rings, E.H.H.M., Delemarre-van de Waal, H.A., van der Grond, J., 2017. Brain structure, executive function and appetitive traits in adolescent obesity. *Pediatr. Obes.* 12 (4), e33–e36. <https://doi.org/10.1111/ijpo.12149>.
- Destrieux, C., Fischl, B., Dale, A., Halgren, E., 2010. Automatic parcellation of human cortical gyri and sulci using standard anatomical nomenclature. *Neuroimage* 53 (1), 1–15. <https://doi.org/10.1016/j.neuroimage.2010.06.010>.
- Elman, J.A., Panizzon, M.S., Hagler, D.J., et al., 2017. Genetic and environmental influences on cortical mean diffusivity. *Neuroimage* 146 (858), 90–99. <https://doi.org/10.1016/j.neuroimage.2016.11.032>.
- Feldstein Ewing, S.W., Bjork, J.M., Luciana, M., 2018. Implications of the ABCD study for developmental neuroscience. *Dev. Cogn. Neurosci.* 32, 161–164. <https://doi.org/10.1016/j.dcn.2018.05.003>.
- Finkelstein, E.A., Trogdon, J.G., Cohen, J.W., Dietz, W., 2009. Annual medical spending attributable to obesity: payer- and service-specific estimates. *Health Aff.* 28 (5), w822–w831. <https://doi.org/10.1377/hlthaff.28.5.w822>.
- Fischl, B., Salat, D.H., Busa, E., et al., 2002. Whole brain segmentation. *Neuron* 33 (3), 341–355. [https://doi.org/10.1016/s0896-6273\(02\)00569-x](https://doi.org/10.1016/s0896-6273(02)00569-x).
- Frank, S., Kullmann, S., Veit, R., 2013. Food related processes in the insular cortex. *Front. Hum. Neurosci.* 7 (August), 499. <https://doi.org/10.3389/fnhum.2013.00499>.
- Fryar, C.D., Carroll, M.D., Ogden, C.L., 2018. Prevalence of overweight, obesity, and severe obesity among adults aged 20 and Over: United States, 1960–1962 through 2015–2016. *NCHS Heal E-Stats* 1 (1), 1–6.
- Garavan, H., Bartsch, H., Conway, K., et al., 2018. Recruiting the ABCD sample: design considerations and procedures. *Dev. Cogn. Neurosci.* 32 (April), 16–22. <https://doi.org/10.1016/j.dcn.2018.04.004>.
- Geserick, M., Vogel, M., Gausche, R., et al., 2018. Acceleration of BMI in early childhood and risk of sustained obesity. *N. Engl. J. Med.* 379 (14), 1303–1312. <https://doi.org/10.1056/NEJMoa1803527>.
- Gordon, E.M., Laumann, T.O., Adeyemo, B., Hunkins, J.F., Kelley, W.M., Petersen, S.E., 2016. Generation and evaluation of a cortical area parcellation from resting-state correlations. *Cereb. Cortex* 26 (1), 288–303. <https://doi.org/10.1093/cercor/bhu239>.
- Guillemot-Legrès, O., Muccioli, G.G., 2017. Obesity-induced neuroinflammation: beyond the hypothalamus. *Trends Neurosci.* 40 (4), 237–253. <https://doi.org/10.1016/j.tins.2017.02.005>.
- Gurnani, M., Birken, C., Hamilton, J., 2015. Childhood obesity: causes, consequences, and management. *Pediatr. Clin. North Am.* 62 (4), 821–840. <https://doi.org/10.1016/j.pcl.2015.04.001>.
- Hagler, D.J., Hutton, S.N., Makowski, C., et al., 2018. Image processing and analysis methods for the Adolescent Brain Cognitive. *bioRxiv* 1–53. <https://doi.org/10.1101/457739>.
- Hales, C., 2017. Prevalence of obesity among adults and youth: United States, 2015–2016 key findings data from the National Health and Nutrition Examination Survey. *NCHS Data Brief* 288. <https://www.cdc.gov/nchs/data/databriefs/db288.pdf>.
- Hao, G., Wang, X., Treiber, F.A., Harshfield, G., Kapuku, G., Su, S., 2018. Body mass index trajectories in childhood is predictive of cardiovascular risk: results from the 23-year longitudinal Georgia Stress and Heart study. *Int. J. Obes.* 42 (4), 923–925. <https://doi.org/10.1038/ijo.2017.244>.
- Hemmingson, E., 2018. Early childhood obesity risk factors: socioeconomic adversity, family dysfunction, offspring distress, and junk food self-medication. *Curr. Obes. Rep.* 7 (2), 204–209. <https://doi.org/10.1007/s13679-018-0310-2>.
- Hill, J.O., Wyatt, H.R., Peters, J.C., 2012. Energy balance and obesity. *Circulation* 126 (1), 126–132. <https://doi.org/10.1161/CIRCULATIONAHA.111.087213>.
- Ho, D., 2011. MatchIt: Nonparametric preprocessing for parametric causal inference. *J. Stat.* <https://doi.org/10.18637/jss.v042.i08>.
- Ho, A.J., Raji, C.A., Becker, J.T., et al., 2010. Obesity is linked with lower brain volume in 700 AD and MCI patients. *Neurobiol. Aging* 31 (8), 1326–1339. <https://doi.org/10.1016/j.neurobiolaging.2010.04.006>.
- Hofmann, W., 2008. Impulsive versus reflective influences on health behavior: a theoretical framework and empirical review. *Health Psychol. Rev.* <https://doi.org/10.1080/17437190802617668>.
- Kaplowitz, P.B., 2008. Link between body fat and the timing of puberty. *Pediatrics* 121 (Supplement), S208–S217. <https://doi.org/10.1542/peds.2007-1813F>.
- Kaufman, J., Birmaher, B., Brent, D., et al., 1997. Schedule for affective disorders and schizophrenia for school-age children-present and lifetime version (K-SADS-PL): initial reliability and validity data. *J. Am. Acad. Child Adolesc. Psychiatry.* <https://doi.org/10.1097/00004583-199707000-00021>.
- Kelsey, M.M., Zaepfel, A., Bjornstad, P., Nadeau, K.J., 2014. Age-related consequences of childhood obesity. *Gerontology* 60 (3), 222–228. <https://doi.org/10.1159/000356023>.
- Kroemer, N.B., Small, D.M., 2016. Fuel not fun: reinterpreting attenuated brain responses to reward in obesity. *Physiol. Behav.* 162, 1–9. <https://doi.org/10.1016/j.physbeh.2016.04.020>.
- Kuczmariski, R.J., Ogden, C.L., Guo, S.S., 2000. CDC Growth Charts for the United States: Methods and Development, Vol 11. <https://doi.org/10.1590/S1516-35982002000600018>, 2002.
- Laurent, J.S., Watts, R., Adise, S., et al., 2019. Associations among body mass index, cortical thickness, and executive function in children. *JAMA Pediatr.* <https://doi.org/10.1001/jamapediatrics.2019.4708>.
- Mendes, N.F., Kim, Y.B., Velloso, L.A., Araújo, E.P., 2018. Hypothalamic microglial activation in obesity: a mini-review. *Front. Neurosci.* (12 November), 1–8. <https://doi.org/10.3389/fnins.2018.00846>.
- Mestre, Z.L., Bischoff-Grethe, A., Eichen, D.M., Wierenga, C.E., Strong, D., Boutelle, K.N., 2017. Hippocampal atrophy and altered brain responses to pleasant tastes among obese compared to healthy weight children. *Int. J. Obes. (May)*, 1–30. <https://doi.org/10.1038/ijo.2017.130>.
- Miller, A.L., Lee, H.J., Lumeng, J.C., 2014. Obesity-associated biomarkers and executive function in children. *Pediatr. Res.* 77 (0), 143–147. <https://doi.org/10.1038/pr.2014.158>.
- Moreno-Lopez, L., Contreras-Rodriguez, O., Soriano-Mas, C., Stamatakis, E.A., Verdejo-Garcia, A., 2016. Disrupted functional connectivity in adolescent obesity. *Neuroimage Clin.* 12, 262–268. <https://doi.org/10.1016/j.nicl.2016.07.005>.
- Perlaki, G., Molnar, D., Smeets, P.A.M., et al., 2018. Volumetric gray matter measures of amygdala and accumbens in childhood overweight/obesity. *PLoS One* 13 (10), 1–17. <https://doi.org/10.1371/journal.pone.0205331>.
- Petersen, A.C., Crockett, L., Richards, M., Boxer, A., 1988. A self-report measure of pubertal status: reliability, validity, and initial norms. *J. Youth Adolesc.* 17 (2), 117–133. <https://doi.org/10.1007/BF01537962>.
- Qian, J., Hastie, T., Friedman, J., Tibshirani, R., Simon, N., 2013. *Glmnet for Matlab*. [URLhttp://www.stanford.edu/~Hast.2013](http://www.stanford.edu/~Hast.2013).
- Radetz, A., Koirala, N., Krämer, J., et al., 2020. Gray matter integrity predicts white matter network reorganization in multiple sclerosis. *Hum. Brain Mapp.* 41 (4), 917–927. <https://doi.org/10.1002/hbm.24849>.
- Rapuno, K.M., Zieselman, A.L., Kelley, W.M., Sargent, J.D., Heatherton, T.F., Gilbert-Diamond, D., 2017. Genetic risk for obesity predicts nucleus accumbens size and responsibility to real-world food cues. *Proc. Natl. Acad. Sci. U. S. A.* 114 (1), 160–165. <https://doi.org/10.1073/pnas.1605548113>.
- Reilly, J.J., Methven, E., McDowell, Z.C., et al., 2003. Health consequences of obesity. *Arch. Dis. Child.* 88 (9), 748–752. <https://doi.org/10.1136/adc.88.9.748>.
- Rolls, E.T., 2011. Taste, olfactory and food texture reward processing in the brain and obesity. *Int. J. Obes. (Lond)* 35 (4), 550–561. <https://doi.org/10.1038/ijo.2010.155>.
- Rolls, E.T., 2015. Taste, olfactory, and food reward value processing in the brain. *Prog. Neurobiol.* 127–128, 64–90. <https://doi.org/10.1016/j.pneurobio.2015.03.002>.
- Ronan, L., Alexander-Bloch, A., Fletcher, P.C., 2019. Childhood obesity, cortical structure, and executive function in healthy children. *Cereb. Cortex* 1–10. <https://doi.org/10.1093/cercor/bhz257>.
- Schempf, S., Van Jaarsveld, C.H.M., Fisher, A., et al., 2018. Variation in the heritability of child body mass index by obesogenic home environment. *JAMA Pediatr.* 172 (12), 1153–1160. <https://doi.org/10.1001/jamapediatrics.2018.1508>.

- Sharkey, R.J., Karama, S., Dagher, A., 2015. Overweight is not associated with cortical thickness alterations in children. *Front. Neurosci.* 9 (February), 1–7. <https://doi.org/10.3389/fnins.2015.00024>.
- Shulman, E.P., Smith, A.R., Silva, K., et al., 2016. The dual systems model: review, reappraisal, and reaffirmation. *Dev. Cogn. Neurosci.* 17, 103–117. <https://doi.org/10.1016/j.dcn.2015.12.010>.
- Stice, E., Yokum, S., 2016. Neural vulnerability factors that increase risk for future weight gain. *Psychol. Bull.* 142 (5), 447–471. <https://doi.org/10.1037/bul0000044>.
- Stice, E., Yokum, S., Bohon, C., Marti, N., Smolen, A., 2010. Reward circuitry responsivity to food predicts future increases in body mass: moderating effects of DRD2 and DRD4. *Neuroimage* 50 (4), 1618–1625. <https://doi.org/10.1016/j.neuroimage.2010.01.081>.
- Stice, E., Yokum, S., Burger, K.S., 2013. Elevated reward region responsivity predicts future substance use onset but not Overweight/Obesity onset. *Biol. Psychiatry* 73 (9), 869–876. <https://doi.org/10.1016/j.biopsych.2012.11.019>.
- Stice, E., Burger, K.S., Yokum, S., 2015. Reward region responsivity predicts future weight gain and moderating effects of the Taq1A allele. *J. Neurosci.* 35 (28), 10316–10324. <https://doi.org/10.1523/JNEUROSCI.3607-14.2015>.
- Turner, B.O., Paul, E.J., Miller, M.B., Barbey, A.K., 2018. Small sample sizes reduce the replicability of task-based fMRI studies. *Commun Biol* 1 (1). <https://doi.org/10.1038/s42003-018-0073-z>.
- Uban, K.A., Horton, M.K., Jacobus, J., et al., 2018. Biospecimens and the ABCD study: rationale, methods of collection, measurement and early data. *Dev. Cogn. Neurosci.* 32 (March), 97–106. <https://doi.org/10.1016/j.dcn.2018.03.005>.
- Vainik, U., Baker, T.E., Dadar, M., et al., 2018. Neurobehavioral correlates of obesity are largely heritable. *Proc Natl Acad Sci* 115 (37), 9312–9317. <https://doi.org/10.1073/pnas.1718206115>.
- Van, Meer F., Van Der, Laan L.N., Charbonnier, L., Viergever, M.A., Adan, R.A.H., 2016. Developmental differences in the brain response to unhealthy food cues : an fMRI study of children and adults 1, 2. *Am. J. Clin. Nutr.* 104 (February), 1515–1522. <https://doi.org/10.3945/ajcn.116.137240.2>.
- Volkow, N.D., Koob, G.F., Croyle, R.T., et al., 2018. The conception of the ABCD study: from substance use to a broad NIH collaboration. *Dev. Cogn. Neurosci.* 32 (April 2017), 4–7. <https://doi.org/10.1016/j.dcn.2017.10.002>.
- Winter, S.R., Yokum, S., Stice, E., Osipowicz, K., Lowe, M.R., 2017. Elevated reward response to receipt of palatable food predicts future weight variability in healthy-weight adolescents. *Am. J. Clin. Nutr.* 105 (4), 781–789. <https://doi.org/10.3945/ajcn.116.141143>.
- Yokum, S., Ng, J., Stice, E., 2011. Attentional Bias to food images associated with elevated weight and future weight gain: an fMRI study. *Obesity* 19 (9), 1775–1783. <https://doi.org/10.1038/oby.2011.168>.
- Yokum, S., Gearhardt, A.N., Harris, J.L., Brownell, K.D., Stice, E., 2014a. Individual differences in striatum activity to food commercials predict weight gain in adolescents. *Obesity* 22 (12). <https://doi.org/10.1002/oby.20882> n/a-n/a.
- Yokum, S., Gearhardt, A.N., Harris, J.L., Brownell, K.D., Stice, E., 2014b. Individual differences in striatum activity to food commercials predict weight gain in adolescents. *Obesity* 22 (12). <https://doi.org/10.1002/oby.20882> n/a-n/a.